



Synthesis, crystal structure, thermal stability, and photoluminescence of a 3-D silver(I) network with twofold interpenetrated dia-f topology

Lu-Lu Han, Ya-Xin Wang, Zhi-Min Guo, Chen Yin, Tuo-Ping Hu, Xing-Po Wang & Di Sun

To cite this article: Lu-Lu Han, Ya-Xin Wang, Zhi-Min Guo, Chen Yin, Tuo-Ping Hu, Xing-Po Wang & Di Sun (2015) Synthesis, crystal structure, thermal stability, and photoluminescence of a 3-D silver(I) network with twofold interpenetrated dia-f topology, Journal of Coordination Chemistry, 68:10, 1754-1764, DOI: [10.1080/00958972.2015.1028380](https://doi.org/10.1080/00958972.2015.1028380)

To link to this article: <http://dx.doi.org/10.1080/00958972.2015.1028380>



Accepted author version posted online: 11 Mar 2015.
Published online: 15 Apr 2015.



Submit your article to this journal [↗](#)



Article views: 77



View related articles [↗](#)




View Crossmark data [↗](#)



Citing articles: 1 View citing articles [↗](#)

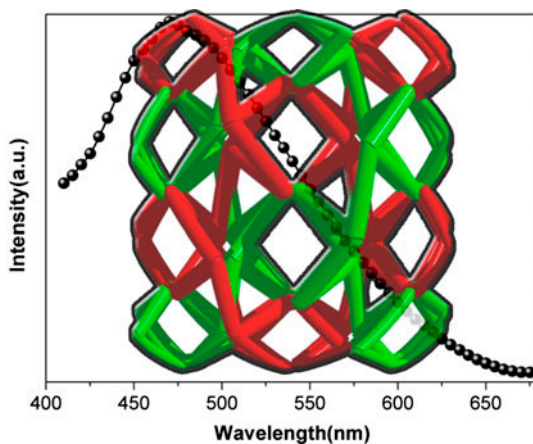
Synthesis, crystal structure, thermal stability, and photoluminescence of a 3-D silver(I) network with twofold interpenetrated dia-f topology

LU-LU HAN[†], YA-XIN WANG[†], ZHI-MIN GUO[†], CHEN YIN[†], TUO-PING HU[‡],
XING-PO WANG[†] and DI SUN^{*†} 

[†]Key Lab for Colloid and Interface Chemistry of Education Ministry, School of Chemistry and Chemical Engineering, Shandong University, Jinan, PR China

[‡]Department of Chemistry, North University of China, Taiyuan, PR China

(Received 3 April 2014; accepted 24 February 2015)



With bpz and *in situ* generated fumaric acid ligands, a new polymer of $[\text{Ag}_2(\text{bpz})_3(\text{fum})]_n$ was synthesized under hydrothermal conditions. It presents a unique twofold interpenetrated 3-D network with a rare **dia-f** topology. If the $\text{Ag}(\text{I})\cdots\text{Ag}(\text{I})$ interaction is included in the simplification of the net, each $\text{Ag}(\text{I})$ is a 4-connected node, thus, a non-interpenetrated 4-connected **upd** net with a point symbol of $\{4.6^3.8^2\}$ is obtained.

A silver(I) coordination polymer with mixed 3,3',5,5'-tetramethyl-4,4'-bipyrazole (bpz) and maleic acid, $[\text{Ag}_2(\text{bpz})_3(\text{fum})]_n$ (**1**, H_2fum = fumaric acid), was synthesized under hydrothermal condition by *in situ* isomerization of maleic acid to fumaric acid and characterized by elemental analysis, IR spectroscopy, powder X-ray diffraction, TGA, and single-crystal X-ray diffraction. The maleic acid *in situ* isomerizes to fumaric acid and participates in the formation of **1**. Topologically, the structure of **1** features a rare 3-connected twofold interpenetrated **dia-f** net with a point symbol of $\{4.14^2\}$. Compound **1** exhibits photoluminescence in the solid state with an emission maximum at 470 nm

*Corresponding author. Email: dsun@sdu.edu.cn

upon excitation at 365 nm at room temperature, which is attributed to intraligand or/and interligand $\pi \rightarrow \pi^*$ transition.

Keywords: Silver; 3,3',5,5'-tetramethyl-4,4'-bipyrazole; Maleic acid

1. Introduction

Recently, coordination polymers (CPs) have attracted attention because of their novel topologies and applications in luminescence, magnetism, sensors, gas adsorption, ion exchange, and catalysis [1–14]. However, it is still a challenge to control the structures of CPs because there are many influencing factors including internal factors such as coordination geometry of central metal, the nature of organic ligand, the ratio of them, and external factors such as pH, temperature, solvent, etc. [15–21]. Ag(I)-based CPs represent an interesting family among CPs. Ag(I) ion is a soft acid that favors coordination of soft bases, such as ligands that contain P, S, and unsaturated nitrogen [22, 23]; its coordination numbers vary from two to six, or even seven and eight, with diverse coordination geometries, including linear, trigonal-planar, tetrahedral, trigonal-pyramidal, square-planar, pyramidal, and octahedral geometries [24–27]. 3,3',5,5'-tetramethyl-4,4'-bipyrazole (bpz) normally appears as an exo-bidentate ligand, whereby the connected metal centers adopt distances between 9.0 and 10.5 Å [28–40]. This ligand possesses some flexibility introduced by the free rotation of the two pyrazolyl rings around the central C–C bond. As indicated by a Cambridge Structure Database survey with the help of ConQuest, version 1.3 [41, 42], 67 coordination compounds based on bpz were found and their torsional angles between the two pyrazolyl rings vary from 54.2° to 129.8°, which can lead to very different conformations (scheme 1). Carboxylic ligands are widely used as the second ligand to diversify the chemical structure because of their diverse coordination modes and abundant hydrogen bonding [43]. Several Ag(I)–bpz CPs have been prepared by incorporating different anions, such as NO_3^- , PO_2F_2^- , ClO_4^- , CF_3SO_3^- , SO_4^{2-} , etc. For example, 1-D polymeric chain $[\text{Ag}(\text{bpz})(\text{NO}_3)\cdot\text{CH}_3\text{OH}]_n$ with methanol of crystallization is involved in hydrogen bonding with NH and NO_3 groups [44], 2-D network $[\text{Ag}_2(\text{bpz})_3(\text{CF}_3\text{CO}_2)_2]_n$ based on interconnected helices [45], and twofold interpenetrated 3-D framework $[\text{Ag}_4(\text{bpz})_4(\text{SO}_4)_2\cdot\text{H}_2\text{O}]_n$ with an uncommon (3,5)-connected **hms** topology [46]. The formations are usually dependent on different small anions. Only a few Ag(I)/bpz/dicarboxylate coordination complexes are reported. For example, 1-D polymeric chain $[\text{Ag}_2(\text{m2CA})(\text{bpz})_2]_n$ (m2CA, isophthalate) features a rope-ladder motif supported by bivalent acid anions [47].

Based on the above consideration and our previous work, in this paper, we report the synthesis, crystal structure, thermal stability, and photoluminescence property of a silver(I)/bipyrazole/dicarboxylate CP, $[\text{Ag}_2(\text{bpz})_3(\text{fum})]_n$, which shows a rare 3-connected twofold interpenetrated **dia-f** net with a point symbol of $\{4.14^2\}$ and emission maximum at 470 nm upon excitation at 365 nm at room temperature.

2. Experimental

2.1. Materials and methods

All reagents and solvents employed were commercially available and used as received. Infrared spectra were recorded on a Nicolet AVATAT FT-IR330 spectrometer with KBr

pellets in the frequency range 4000–400 cm^{-1} . Elemental analyses (C, H and N) were determined on a CE instrument EA 1110 analyzer. Photoluminescence measurements were performed on a Hitachi F-7000 fluorescence spectrophotometer with solid powder on a 1 cm quartz round plate. Thermogravimetric (TG) curves were measured from 30 to 800 $^{\circ}\text{C}$ on a NETZSCH TG 209 F1 Iris® TG Analyzer at a heating rate of 10 $^{\circ}\text{C min}^{-1}$ under N_2 (20 mL min^{-1}). Powder X-ray diffraction (PXRD) measurements were recorded on a D/Max-2500 X-ray diffractometer using $\text{Cu-K}\alpha$ radiation.

2.2. Synthesis of $[\text{Ag}_2(\text{bpz})_3(\text{fum})]_n$ (**1**)

A mixture of Ag_2O (11.6 mg, 0.05 mmol), bpz (19 mg, 0.1 mmol), maleic acid (11.6 mg, 0.1 mmol), 5 mL H_2O , and 0.15 mL pyridine was heated to 90 $^{\circ}\text{C}$ for 8 h in a 25 mL Teflon-lined reaction vessel, kept at 90 $^{\circ}\text{C}$ for 50 h, then slowly cooled to 30 $^{\circ}\text{C}$ in 10 h. The pH values of the system were 6.06 and 6.10 before and after the hydrothermal reaction, respectively. Colorless block crystals of **1** were isolated by filtration, washed with H_2O , and dried in air. Anal. Calcd (found) for $\text{C}_{17}\text{H}_{22}\text{AgN}_6\text{O}_2$: C, 45.35 (45.79); H, 4.92 (4.88); N, 18.66 (18.59)%. IR (KBr): $\nu(\text{cm}^{-1}) = 3144(\text{w}), 2920(\text{w}), 2799(\text{w}), 1578(\text{s}), 1416(\text{w}), 1364(\text{s}), 1299(\text{w}), 1160(\text{w}), 1026(\text{w}), 972(\text{w}), 863(\text{w}), 778(\text{w}), 662(\text{w}), 526(\text{w}), 497(\text{w}), 432(\text{w})$.

When the synthesis was done with fumaric acid, abundant precipitate was obtained. After the precipitate was washed with ethanol, most precipitate dissolved and there were very few crystals left at the bottom. Cell parameters of them determined by X-ray diffraction were the same as those of **1**. But the crystal obtained using fumaric acid was very small and the yield was much lower than using maleic acid.

2.3. X-ray crystallography

Single crystals of **1** with appropriate dimensions were chosen under an optical microscope and quickly coated with high vacuum grease (Dow Corning Corporation) before being mounted on a glass fiber for data collection. Data for them were collected on a Bruker Apex II CCD diffractometer with graphite-monochromated $\text{Mo-K}\alpha$ radiation ($\lambda = 0.71073 \text{ \AA}$). A preliminary orientation matrix and unit cell parameters were determined from 3 runs of 12 frames each, each frame corresponds to a 0.5° scan in 5 s, followed by spot integration and least-squares refinement. For **1**, data were measured using ω scans of 0.5° per frame for 10 s until a complete hemisphere had been collected. Cell parameters were retrieved using SMART software and refined with SAINT on all observed reflections [48]. Data reduction was performed with the SAINT software and corrected for Lorentz and polarization effects. Absorption corrections were applied with SADABS [48]. The highest possible space group was chosen. The structure was solved by direct methods using SHELXS-97 [49] and refined on F^2 by full-matrix least-squares procedure with SHELXL-97 [50]. Atoms were located from iterative examination of difference F-maps following least-squares refinements of the earlier models. Hydrogens were placed in calculated positions and included as riding with isotropic displacement parameters 1.2–1.5 times U_{eq} of the attached C or N. All structures were examined using the Addsym subroutine of PLATON [51] to assure that no additional symmetry could be applied to the models. The fum ion was disordered in two slightly different orientations with a major orientation of 70%. To assist refinement of the disordered moieties in **1**, SIMU was applied to restrain the similar thermal parameters on adjacent atoms in disordered moieties. The very small void volume of 51 \AA^3 in one unit cell

Table 1. Crystallographic data and details of diffraction experiments of **1** and **2**.

Empirical formula	C ₁₇ H ₂₂ AgN ₆ O ₂
Formula weight	450.28
Temperature/K	298(2)
Crystal system	Tetragonal
Space group	I4 ₁ /acd
a/Å	23.3823(14)
c/Å	28.1857(17)
Volume/Å ³	15410.0(13)
Z	32
ρ_{Calcd} g/cm ³	1.553
μ /mm	1.070
F(0 0 0)	7328.0
Crystal size/mm ³	0.15 × 0.06 × 0.06
2 θ range for data collection	3.48–50°
Index ranges	–20 ≤ h ≤ 27, –27 ≤ k ≤ 25, –33 ≤ l ≤ 32
Reflections collected	36,353
Independent reflections	3397[R(int) = 0.0523]
Data/restraints/parameters	3397/6/268
Goodness-of-fit on F ²	0.970
Final R indexes [I ≥ 2σ(I)]	R ₁ = 0.0338, wR ₂ = 0.0782
Final R indexes [all data]	R ₁ = 0.0537, wR ₂ = 0.0897
Largest diff. peak/hole/e Å ^{–3}	0.43/–0.32

compared to the total cell unit volume of 15410.0(13) Å³ indicates that nothing could be assigned in such a high symmetry crystal. Small residual voids in a structure may go undetected when smeared since peak search programs are not designed to locate maxima on density ridges. Voids of 40 Å³ may accommodate one H₂O, but 51 Å³ in one unit cell (Z = 32) corresponds to 1/32 H₂O molecule per formula of **1**, which does not make sense in this structure. Topological analysis of the complex was performed with the program package TOPOS [52]. Pertinent crystallographic data collection and refinement parameters are in table 1. Selected bond lengths and angles are presented in table 2. The hydrogen bond parameters are in table 3.

Table 2. Selected bond lengths (Å) and angles (°) for **1**.

Ag1–N1	2.265(3)	Ag1–N5	2.246(3)	Ag1–N4 ^a	2.388(3)
N5–Ag1 – N1	139.75(11)	N1–Ag1 – N4 ^a	106.91(11)	N5–Ag1 – N4 ^a	98.24(11)

Symmetry codes: ^a–y + 5/4, x + 1/4, –z + 3/4.

Table 3. The hydrogen bond geometry for **1**.

D–H⋯A	D–H	H⋯A	D⋯A	D–H⋯A
N2–H2⋯O2 ^b	0.86	2.23	2.963 (8)	142.5
N2–H2⋯O1 ^b	0.86	2.24	3.058 (12)	157.8
N3–H3⋯O1 ^c	0.86	1.90	2.741 (14)	163.9
N6–H6⋯O2 ^b	0.86	1.91	2.683 (11)	149.2

Symmetry codes: ^b–x + 1, –y + 1, –z + 1; ^cy – 1/4, –x + 5/4, –z + 3/4.

3. Results and discussion

3.1. Structure description of $[Ag_2(bpz)_3(fum)]_n$

Single-crystal X-ray diffraction analysis reveals that **1** crystallizes in the tetragonal space group $I4_1/acd$ and the asymmetric unit contains one crystallographically independent Ag(I), one and a half bpz, and a half of uncoordinated fum anion. The coordination environment of **1** is shown in figure 1(a). Ag(I) is 3-coordinated by three nitrogens from three different bpz ligands in triangular coordination geometry with the maximum bond angle of $139.75(11)^\circ$. The Ag–N bond lengths range from 2.246(3) to 2.388(3) Å (Ag1–N1 = 2.265(3), Ag1–N5 = 2.246(3), and Ag1–N4ⁱ = 2.388(3)). Symmetry code: (i) $-y + 5/4, x + 1/4,$

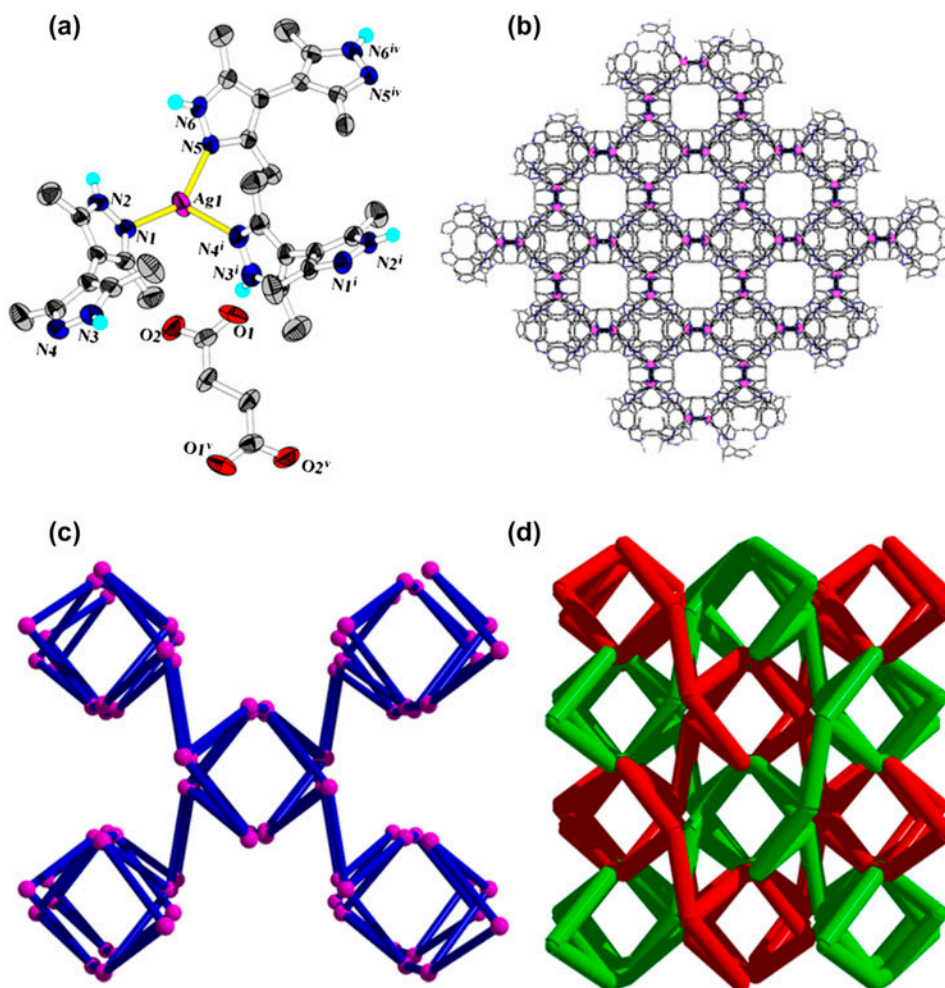


Figure 1. (a) Coordination environment around the central Ag(I) in **1** with only Ag(I) coordination environment labeled and 30% thermal ellipsoid. (b) Ball-and-stick representation of the 3-D framework (purple ball: Ag; blue ball: N; and gray ball: C). (c) Ball-and-stick view of simplified single **dia-f** net. (d) Schematic view of the simplified twofold interpenetrated network (networks individually colored) (see <http://dx.doi.org/10.1080/00958972.2015.1028380> for color version).

$-z + 3/4$), which are comparable with the reported values such as in $[\text{Ag}(\text{OAc})(\text{bpz})_2]_n \cdot 5.4 \text{ H}_2\text{O}$ in which the Ag–N bond lengths range from 2.214(2) to 2.226(2) Å [47]. One bpz has a C2 axis along the midpoint of C13–C13^{iv} bond (symmetry code: (iv) $-x + 1.5, y, -z + 1$). The inter-pyrazole dihedral angles for two different bpz ligands are 82.18(19) and 73.64(2)°, respectively. The shortest Ag(I)⋯Ag(I) separation is 3.0608(6) Å, which is shorter than the sum of Ag(I) van der Waals radii (3.44 Å), indicating the presence of ligand-unsupported argentophilicity. This distance is comparable to the 3.095(1) Å in $[\text{Ag}(\text{PCy}_3)(\text{O}_2\text{CCF}_3)_2]$ and 2.938(1) Å in $[\text{Ag}_2(\mu\text{-dcpm})_2](\text{PF}_6)_2$ (dcpm = bis(dicyclohexylphosphino) methane) [53–57]. The bpz ligands with an exo-bidentate mode extend the Ag(I) centers into a 3-D framework [figure 1(b)] in which the fum did not participate in the resultant network and only acted as a counter-anion connected with the Ag(I) network by N–H⋯O hydrogen bonds (N⋯O: 2.683(11)–3.058(12) Å; table 3). Comparing with the similar complexes but using aromatic dicarboxylate [47], for example, $[\text{Ag}(\text{Hp2CA})(\text{bpz})_n]$ (Hp2CA, terephthalic acid monoanion) and $[\text{Ag}_2(\text{m2CA})(\text{bpz})_2]_n$ (m2CA, isophthalate) have 2-D and 1-D networks, respectively. This structure shows a higher dimensionality though the fum did not coordinate with Ag(I).

In order to understand the complicated 3-D framework, topology of **1** was analyzed using TOPOS software. The bpz bridging ligands are omitted because of their linear linkage and each Ag linked by three bpz ligands is treated as a 3-connecting node, so the 3-D framework can be simplified to a rare 3-connected $\{4.14^2\}$ net, which is assigned to a **dia-f** topology, as displayed in figure 1(c). To avoid the large space within the crystal packing, two equivalent **dia-f** nets are twofold interpenetrated [figure 1(d)] and interlocked with each other through Ag(I)⋯Ag(I) interaction. The interpenetration can be classified as Class IIa, which means that two identical interpenetrated nets are generated by means of space group interpenetration symmetry element, here an inversion center, and no other interpenetrating translations are allowed in this kind of interpenetration. The present net is different from the regular **dia-f** net, whose symmetrical configuration is normally $I4_1/\text{amd}$ of the tetragonal cell [58]. Alternatively, if the Ag(I)⋯Ag(I) interaction is included in the simplification of the net, each Ag(I) becomes a 4-connected node, thus a non-interpenetrated 4-connected **upd** net with a point symbol of $\{4.6^3.8^2\}$ is produced.

3.2. Synthesis and IR spectrum discussion

Complex **1** was prepared by the reaction of Ag_2O with bpz and maleic acid under hydrothermal conditions. However, after heating at 90 °C for about 50 h, maleic acid isomerized to fumaric acid based on single-crystal X-ray diffraction analysis. The maleic acid *in situ* isomerized to fumaric acid may be catalyzed by acid [59]. When fumaric acid was used, **1** was also obtained but with very low yield. IR spectra of **1** show characteristic absorptions mainly attributed to the asymmetric (ν_{as} : 1578 cm^{-1}) and symmetric (ν_{s} : ca. 1364 cm^{-1}) stretching vibrations of the carboxylic groups which correspond to the $\text{Na}_2(\text{fum})$ [60]; this also shows the isomerization of maleic acid. Separation between the antisymmetric and symmetric carboxylate stretching in the IR spectrum is 214 cm^{-1} , which is a little large, and may be “pseudo-unidentate” coordination of fum ions because of the hydrogen bridges [61]. No band at 1690–1730 cm^{-1} indicates complete deprotonation of the carboxylic groups, consistent with charge balance.

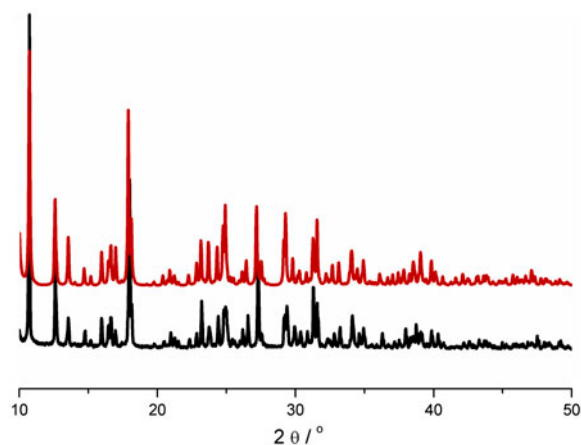


Figure 2. PXRD patterns for **1** (upper line: calculated from single-crystal X-ray diffraction data; bottom line: as synthesized solids).

3.3. PXRD and thermal analysis

PXRD has been used to check the phase purity of the bulk samples in the solid state. For **1**, the measured PXRD patterns closely match the simulated patterns generated from the results of single-crystal diffraction data (figure 2), indicating pure products. The differences in intensity may be due to the preferred orientation of the crystalline powder samples.

The TG analysis was performed in N_2 (100 mL min^{-1}) on **1**. The temperature was ramped at a rate of $10 \text{ }^\circ\text{C min}^{-1}$ from 30 to $800 \text{ }^\circ\text{C}$. The TG curves are shown in figure 3. The first weight loss of 12.92% in the temperature range of 30–234 $^\circ\text{C}$ indicates the loss of one fum acid per formula (Calcd: 12.89%), then the second weight loss of 64.01% at about 350 $^\circ\text{C}$ indicates the loss of three bpz ligands (Calcd: 63.29%) with accompanying collapse of the host framework.

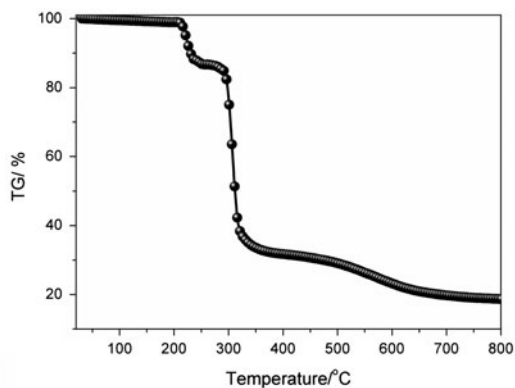


Figure 3. TGA curve for **1**.

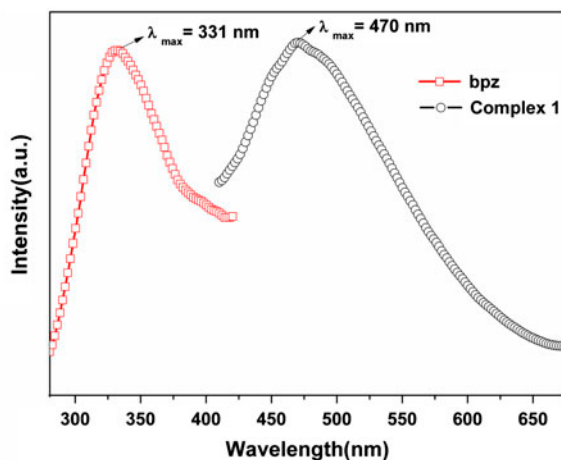
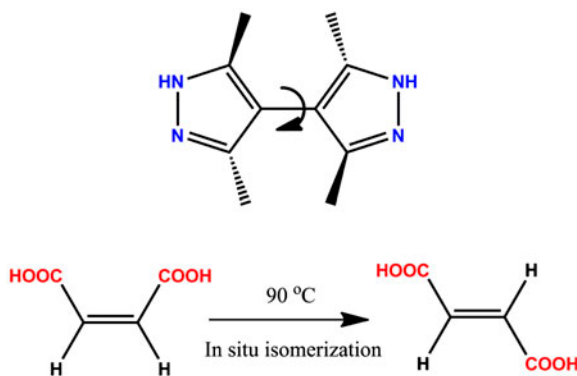


Figure 4. Emission spectra of free bpz and **1** at 298 K.

3.4. Photoluminescence properties

The solid-state photoluminescence spectrum for **1** at room temperature is shown in figure 4. The free bpz displays photoluminescence with emission maximum at 331 nm. These peaks originate from the $\pi^* \rightarrow n$ or $\pi^* \rightarrow \pi$ transitions [62, 63]. Complex **1** exhibits photoluminescence with an emission maximum at 470 nm, upon excitation at 365 nm at room temperature. The observed emission of **1** is assigned to intraligand or/and interligand $\pi \rightarrow \pi^*$ transitions because a similar emission is observed for the free bpz and **1**. From the literature, the emission of dicarboxylate belongs to $\pi^* \rightarrow n$ transition which is very weak compared to that of the $\pi^* \rightarrow \pi$ transition of bpz, so the dicarboxylate almost has no contribution to the fluorescent emission of **1** [64]. The enhanced emission intensity of **1** compared to bpz was attributed to ligand coordination to the metal center, which effectively increases the rigidity of the ligand and reduces the loss of energy by radiationless decay [65].



Scheme 1. The organic ligand used in the construction of **1**.

4. Conclusion

A new silver(I) CP was constructed from bpz and *in situ* generated maleic acid ligands under hydrothermal conditions. It presents a unique twofold interpenetrated 3-D network with a rare **dia-f** topology. Including the Ag(I)⋯Ag(I) interaction in the simplification of the net, each Ag(I) becomes a 4-connected node, thus a non-interpenetrated 4-connected **upd** net with a point symbol of {4.6³.8²} is obtained. Its photoluminescence at room temperature and thermal stability were also investigated.

Supplementary material

For **1**, further details on the crystal structure investigations can be obtained from the Cambridge Crystallographic Data Center, CCDC, 12 Union Road, Cambridge CB2 1EZ, UK. Copies of the data can be obtained free of charge on quoting the depository numbers CCDC-987588 (Fax: +44 1223 336 033; E-mail: deposit@ccdc.cam.ac.uk, <http://www.ccdc.cam.ac.uk>).

Disclosure statement

No potential conflict of interest was reported by the authors.

Funding

This work was supported by NSFC [grant number 21201110]; China Postdoctoral Science Foundation [grant number 2013T60663]; Research Award Fund for Outstanding Middle-aged and Young Scientist of Shandong Province [grant number BS2013CL010]; Dr T.P. Hu thanks the International Scientific and Technological Cooperation Projects of Shanxi Province [grant number 2011081022].

ORCID

Di Sun  <http://orcid.org/0000-0001-5966-1207>

References

- [1] H. Wu, J. Yang, Z.M. Su, S.R. Batten, J.F. Ma. *J. Am. Chem. Soc.*, **133**, 11406 (2011).
- [2] W.S. Liu, T.Q. Jiao, Y.Z. Li, Q.Z. Liu, M.Y. Tan, H. Wang, L.F. Wang. *J. Am. Chem. Soc.*, **126**, 2280 (2004).
- [3] M. O'Keeffe, O.M. Yaghi. *Chem. Rev.*, **112**, 675 (2012).
- [4] K.K. Tanabe, C.A. Allen, S.M. Cohen. *Angew. Chem. Int. Ed.*, **49**, 9730 (2010).
- [5] C.Y. Su, Y.P. Cai, C.L. Chen, M.D. Smith, W. Kaim, H.C. zur Loye. *J. Am. Chem. Soc.*, **125**, 8595 (2003).
- [6] D.Q. Yuan, D. Zhao, D.J. Timmons, H.C. Zhou. *Chem. Sci.*, **2**, 103 (2011).
- [7] Y.F. Bi, X.T. Wang, W.P. Liao, X.F. Wang, X.W. Wang, H.J. Zhang, S. Gao. *J. Am. Chem. Soc.*, **131**, 11650 (2009).
- [8] X.P. Zhou, J. Liu, S.Z. Zhan, J.R. Yang, D. Li, K.M. Ng, R.W.Y. Sun, C.M. Che. *J. Am. Chem. Soc.*, **134**, 8042 (2012).
- [9] X.P. Zhou, M. Li, J. Liu, D. Li. *J. Am. Chem. Soc.*, **134**, 67 (2012).
- [10] X.J. Kong, L.S. Long, Z. Zheng, R.B. Huang, L.S. Zheng. *Acc. Chem. Res.*, **43**, 201 (2010).
- [11] E.B. Rusanov, V.V. Ponomarova, V.V. Komarchuk, H. Stoeckli-Evans, E. Fernandez Ibanez, F. Stoeckli, J. Sieler, K.V. Domasevitch. *Angew. Chem. Int. Ed.*, **42**, 2499 (2003).
- [12] Z. Yin, Q.X. Wang, M.H. Zeng. *J. Am. Chem. Soc.*, **134**, 4857 (2012).
- [13] B. Chen, S. Xiang, G. Qian. *Acc. Chem. Res.*, **43**, 1115 (2010).

- [14] M. Yoshizawa, J.K. Klosterman, M. Fujita. *Angew. Chem. Int. Ed.*, **48**, 3418 (2009).
- [15] X.C. Huang, J.P. Zhang, X.M. Chen. *J. Am. Chem. Soc.*, **126**, 13218 (2004).
- [16] X.C. Huang, J.P. Zhang, Y.Y. Lin, X.M. Chen. *Chem. Commun.*, 2232 (2005).
- [17] Z.Q. Wang, V.C. Kravtsov, M.J. Zaworotko. *Angew. Chem. Int. Ed.*, **44**, 2877 (2005).
- [18] J. He, Y.G. Yin, X.C. Huang, D. Li. *Inorg. Chem. Commun.*, **9**, 205 (2006).
- [19] B. Zhao, P. Cheng, X.-Y. Chen, C. Cheng, W. Shi, D.Z. Liao, S.P. Yan, Z.H. Jiang. *J. Am. Chem. Soc.*, **126**, 3012 (2004).
- [20] X.M. Zhang. *Coord. Chem. Rev.*, **249**, 1201 (2005).
- [21] J.P. Zhang, X.M. Chen. *Chem. Commun.*, 1689 (2006).
- [22] L. Carlucci, G. Ciani, D.W.v. Gudenberg, D.M. Proserpio. *Inorg. Chem.*, **36**, 3812 (1997).
- [23] O.S. Jung, S.H. Park, C.H. Park, J.K. Park. *Chem. Lett.*, **28**, 923 (1999).
- [24] G. Férey, C. Mellot-Draznieks, C. Serre, F. Millange. *Acc. Chem. Res.*, **38**, 217 (2005).
- [25] D. Bradshaw, J.B. Claridge, E.J. Cussen, T.J. Prior, M.J. Rosseinsky. *Acc. Chem. Res.*, **38**, 273 (2005).
- [26] F. Nouar, J.F. Eubank, T. Bousquet, L. Wojtas, M.J. Zaworotko, M. Eddaoudi. *J. Am. Chem. Soc.*, **130**, 1833 (2008).
- [27] D.P. Dong, Z.G. Sun, F. Tong, Y.Y. Zhu, K. Chen, C.Q. Jiao, C.L. Wang, C. Li, W.N. Wang. *CrystEngComm*, **13**, 3317 (2011).
- [28] I. Boldog, E.B. Rusanov, A.N. Chernega, J. Sieler, K.V. Domasevitch. *Angew. Chem. Int. Ed.*, **40**, 3435 (2001).
- [29] I. Boldog, E.B. Rusanov, J. Sieler, K.V. Domasevitch. *New J. Chem.*, **28**, 756 (2004).
- [30] H. Huang, Q.H. Jin, S.Y. Yu, H.W. Ma, S.H. Li, H.P. Huang, K.B. Yu. *Z. Kristallogr. - New Cryst. Struct.*, **218**, 443 (2003).
- [31] P.V. Ganesan, C.J. Kepert. *Chem. Commun.*, 2168 (2004).
- [32] I. Boldog, J. Sieler, K.V. Domasevitch. *Inorg. Chem. Commun.*, **6**, 769 (2003).
- [33] I. Boldog, E.B. Rusanov, J. Sieler, S. Blaurock, K.V. Domasevitch. *Chem. Commun.*, 740 (2003).
- [34] P.E. Kruger, B. Moubaraki, G.D. Fallon, K.S. Murray. *J. Chem. Soc., Dalton Trans.*, 713 (2000).
- [35] V.V. Ponomarova, V.V. Komarchuk, I. Boldog, A.N. Chernega, J. Sieler, K.V. Domasevitch. *Chem. Commun.*, 436 (2002).
- [36] E.B. Rusanov, V.V. Ponomarova, V.V. Komarchuk, H. Stoeckli-Evans, E. Fernandez-Ibañez, F. Stoeckli, J. Sieler, K.V. Domasevitch. *Angew. Chem. Int. Ed.*, **42**, 2499 (2003).
- [37] V.V. Komarchuk, V.V. Ponomarova, H. Krautscheid, K.V. Domasevitch. *Z. Anorg. Allg. Chem.*, **630**, 1413 (2004).
- [38] I. Boldog, E.B. Rusanov, A.N. Chernega, J. Sieler, K.V. Domasevitch. *Polyhedron*, **20**, 887 (2001).
- [39] I. Boldog, E.B. Rusanov, A.N. Chernega, J. Sieler, K.V. Domasevitch. *J. Chem. Soc., Dalton Trans.*, 893 (2001).
- [40] P.E. Kruger, G.D. Fallon, B. Moubaraki, K.S. Murray. *J. Chem. Soc., Chem. Commun.*, 1726 (1992).
- [41] F.H. Allen. *Acta Crystallogr., Sect. B: Struct. Sci.*, **58**, 380 (2002).
- [42] Cambridge Structure Database search. *CSD Version 5.28 (November 2006) with 20 updates (January 2007–May 2014)*, Cambridge, UK (2006).
- [43] C. Volkringer, T. Loiseau, N. Guillou, G. Férey, M. Haouas, F. Taulelle, N. Audebrand, I. Margiolaki, D. Popov, M. Burghammer, C. Riekel. *Cryst. Growth Des.*, **9**, 2927 (2009).
- [44] I. Boldog, E.B. Rusanov, A.N. Chernega, J. Sieler, K.V. Domasevitch. *Polyhedron*, **20**, 887 (2001).
- [45] K.V. Domasevitch, I. Boldog, E.B. Rusanov, J. Hunger, S. Blaurock, M. Schröder, J. Sieler. *Z. Anorg. Allg. Chem.*, **631**, 1095 (2005).
- [46] L.Y. Du, W.J. Shi, L. Hou, Y.Y. Wang, Q.Z. Shi, Z.H. Zhu. *Inorg. Chem.*, **52**, 14018 (2013).
- [47] J. Hunger, H. Krautscheid, J. Sieler. *Cryst. Growth Des.*, **9**, 4613 (2009).
- [48] Bruker. *SMART, SAINT and SADABS*, Bruker AXS Inc., Madison, WI (1998).
- [49] G.M. Sheldrick. *SHELXS-97, Program for X-ray Crystal Structure Determination*, University of Gottingen, Gottingen, Germany (1997).
- [50] G.M. Sheldrick. *SHELXL-97, Program for X-ray Crystal Structure Refinement*, University of Gottingen, Gottingen, Germany (1997).
- [51] A.L. Spek. *Implemented as the PLATON Procedure, a Multipurpose Crystallographic Tool*, Utrecht University, Utrecht (1998).
- [52] V.A. Blatov. *Struct. Chem.*, **23**, 955 (2012). TOPOS software Available online at: <http://www.topos.samsu.ru>.
- [53] A. Bondi. *J. Phys. Chem.*, **68**, 441 (1964).
- [54] P. Pyykkö. *Chem. Rev.*, **97**, 597 (1997).
- [55] J.P. Zhang, Y.B. Wang, X.C. Huang, Y.Y. Lin, X.M. Chen. *Chem. Eur. J.*, **11**, 552 (2005).
- [56] L. Ray, M.M. Shaikh, P. Ghosh. *Inorg. Chem.*, **47**, 230 (2008).
- [57] C.M. Che, M.C. Tse, M.C.W. Chan, K.K. Cheung, D.L. Phillips, K.H. Leung. *J. Am. Chem. Soc.*, **122**, 2464 (2000).
- [58] Y.M. Xie, Z.G. Zhao, X.Y. Wu, Q.S. Zhang, L.J. Chen, F. Wang, S.C. Chen, C.Z. Lu. *J. Solid State Chem.*, **181**, 3322 (2008).
- [59] K. Nozaki, R. Ogg Jr. *J. Am. Chem. Soc.*, **63**, 2583 (1941).

- [60] E.Y. Ionashiro, F.J. Caires, A.B. Siqueira, L.S. Lima, C.T. Carvalho. *J. Therm. Anal. Calorim.*, **108**, 1183 (2012).
- [61] G.B. Deacon, R.J. Phillips. *Coord. Chem. Rev.*, **33**, 227 (1980).
- [62] J. He, J.X. Zhang, G.P. Tan, Y.G. Yin, D. Zhang, M.H. Hu. *Cryst. Growth Des.*, **7**, 1508 (2007).
- [63] X. Shi, G.S. Zhu, X.H. Wang, G.H. Li, Q.R. Fang, X.J. Zhao, G. Wu, G. Tian, M. Xue, R.W. Wang, S.L. Qiu. *Cryst. Growth Des.*, **5**, 341 (2005).
- [64] C.Y. Xu, Q.Q. Guo, X.J. Wang, H.W. Hou, Y.T. Fan. *Cryst. Growth Des.*, **11**, 1869 (2011).
- [65] V.W.W. Yam. *Acc. Chem. Res.*, **35**, 555 (2002).